Design, Regiospecific Green Synthesis, Chemical Computational Analysis, and Antimicrobial Evaluation of Novel Phthalazine Heterocycles

Sameh A. Rizk,[a] Salwa S. Abdelwahab,[b]* and Azza A. El-Badawy[a]

[a]Chemistry Department, Faculty of Science, Ain Shams University, Cairo, Egypt, 11566
[b]Faculty of Pharmaceutical Sciences and Pharmaceutical Industries, Future University in Egypt, Cairo, Egypt, 11835
*E-mail: salwa_elsayed@ymail.com

Received December 10, 2018
DOI 10.1002/jhet.3622
Published online 30 July 2019 in Wiley Online Library (wileyonlinelibrary.com).

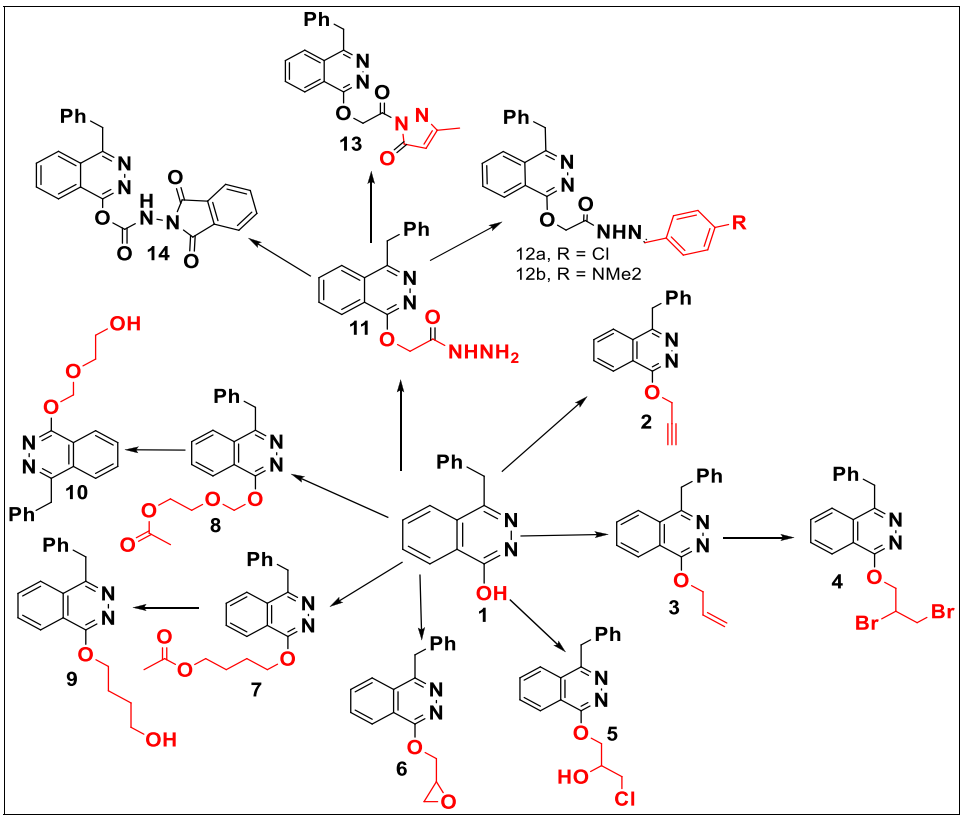

Phthalazines have received considerable attention for their wide antimicrobial activity. Regiospecific nucleophilic attack of 4-benzylphthalazin-1-ol by the 1-oxo rather than the aza group on different alkyl halides gave novel phthalazine heterocyclic derivatives. Moreover, a variety of nucleosides bonded to electron-withdrawing groups were synthesized using 4-benzylphthalazine-1-ol. The density functional theory has been used to investigate the electronic structure of the synthesized compounds. All of the synthesized derivatives showed remarkable activity when tested against Gram-positive and Gram-negative bacteria, *Aspergillus niger*, and *Candida albicans*. The reactivity of these nucleosides was expected to arise from their bonding with the lone pair of N-atom of the macromolecules of bacteria. These bonding were expected to inhibit the enzyme by forming highly stable complex with lower highest occupied molecular orbital energy. The structures of these synthesized derivatives were established by Fourier transform infrared, ^{1}H-NMR, and ^{13}C-NMR spectroscopic evidence.

INTRODUCTION

N-Heterocycles are one of the most important bioactive molecules that were found to have wide applicability [1–5]. Benz-fused pyridazines have gained extensive interest because of their exciting biological properties and have been proven to display appreciable broad spectrum in natural compounds [6–10]. It also acts as a center structure for different bioactive molecules because of its easy fictionalization at different substitution patterns and their roles as pharmacophore [11,12]. Some of *O*-alkyl-phthalazine derivatives were monitored *in vitro* for their antimicrobial effect, and the energy variance between the highest occupied molecular orbital (HOMO) and the lowest unoccupied molecular orbital (LUMO) plays a significant role in the electronic studies

of these molecules by quantum chemical calculations that reflects the relation between delocalization, electron distribution, and chemical reactivity with kinetic stability of the compound [13–17]. Phthalazine derivatives were announced to acquire anticonvulsant [18], antitumor [19], antihypertensive, antithrombotic [20], antidiabetic [21], antitrypanosomal [22], anti-inflammatory [23], cardiotonic [24], and vasorelaxant [25] activities. Therefore, various strategies have been accounted for the synthesis of phthalazine derivatives [26–31]. Regardless of the detailed manufactured strategies, the development of innovative proficient synthesis of phthalazine derivatives is considered an exciting trial [32]; the newest of *O*-substituted-4-benzylphthalazin-1-ol possessing different alkyl groups bound *via* acetyl-flexible linker as anticancer agents was synthesized by incorporation of methylene (CH_2) domains bridge at C-4 position of the phthalazine moiety to afford a litheness that increase their anticancer activity against three human tumor cells [33,34]. In addition, phthalazine-1-ol and its derivatives were bis-phenol-like monomers that can be polymerized with the activated aryl dihalide monomers to give amorphous polymers with high glass transition temperature and excellent thermostability, which are soluble in common organic solvents [35–37]. 4-Benzylphthalazin-1-ol skeleton is considered as intermediates in the construction of bioactive phthalazine derivatives, and its synthesis has been well discussed in recent review paper [38]. So, we designed a specific simple program aiming to construct a new hither to unreported congener using 4-benzyl phthalazine-1-ol synthetic intermediate moiety in a single molecular framework, which is a unique key precursor designing new, potent, selective agent; the novel synthesized derivatives show crucial effect for antimicrobial evaluation.

Scheme 1. Synthesis route for compound **1**.

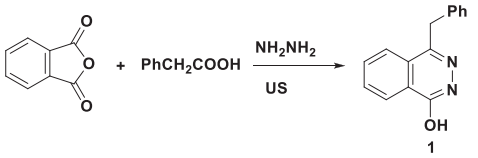

RESULTS AND DISCUSSION

Chemistry. The newly synthesized 4-benzyl-phthalazin-1-ol **1** was initiated from a one-pot strategy ultrasonic reaction of phthalic anhydride, phenylacetic acid, and hydrazine hydrate. Structural elucidations of compound **1** were based on correct spectroscopic data as listed in the Experimental section (Scheme 1). The proposal mechanistic equations of the 4-benzylphthalazin-1-ol are outlined in Scheme 2.

The synthesis of 1-benzyl-4-(prop-2-yn-1-yloxy) phthalazine **2** was emanated from the reaction of phthalazine-1-ol **1** with 3-bromopropyne in the existence of K_2CO_3 anhydrous in dry acetone. Utilizing allyl bromide as an alternative alkylating agent in an analogous way under the same condition afforded the 1-(allyloxy)-4-benzylphthalazine **3**. The alkylation reaction was achieved *via* SN^2 mechanism. In general, IR spectra of **2** and **3** exhibited two absorptions bands at 3248 and 3127 cm^{-1} characteristic for ν_{CH} of alkynyl and alkenyl groups respectively and the absence of any bands in the carbonyl region that proved that the reaction took place *via* *O*-alkylation to afford the *O*-alkyl-phthalazine derivatives.

Meanwhile, ^{1}H-NMR revealed the absence of OH functional group. In order to investigate the improvement in biological activity upon insertion of halogen moieties, therefore, compound **3** was allowed to react with bromine in carbon tetrachloride as a solvent to afford the desired product 1-benzyl-4-(2,3-dibromopropoxy) phthalazine **4** (Scheme 3). In the intervening time, 1-benzyl-4-(oxiran-2-ylmethoxy) phthalazine **6** was obtained *via* the interaction of phthalazine-1-ol **1** with epichlorohydrin in anhydrous

Scheme 2. The proposal mechanistic equations of compound **1**.

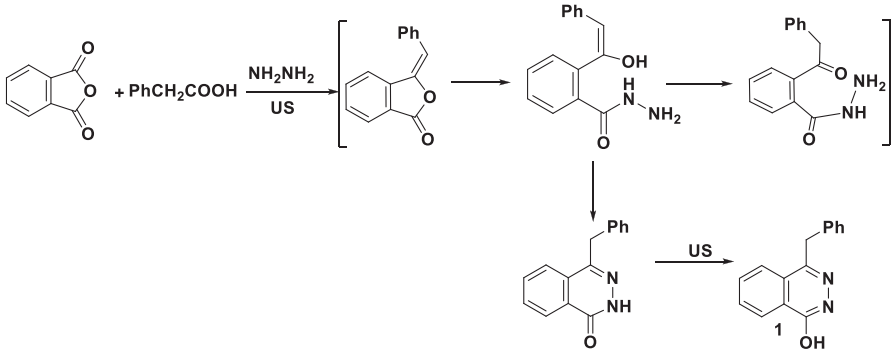

Scheme 3. Synthesis route for compounds **2**–**4**.

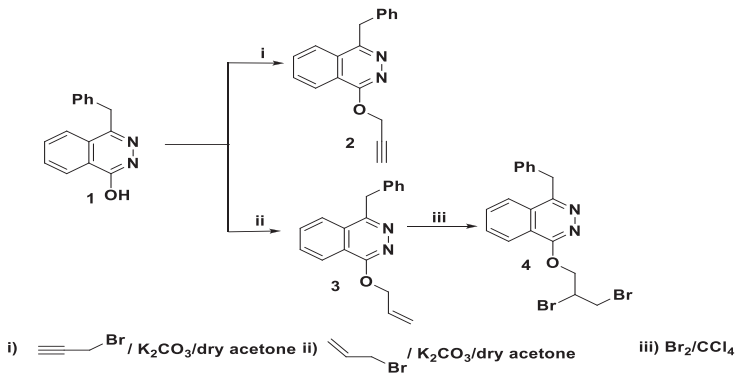

K_2CO_3 in dry dimethylformamide (DMF) *via* the true intermediate **5** that was isolated.

Compound **6** was investigated *via* IR spectrum that displayed bands at 1245, 930, and 830 cm^{-1}characteristics for symmetric and asymmetric ν_{C-O} of epoxide group respectively that indicated the formation of *O*-alkyloxirane product **6** (Scheme 4). The reaction occurred *via* ring opening–ring closure of the oxirane nucleus and not by SN^2 as in the case of the alkyl halide, for example, 1,3-dichloro-propan-2-ol. Formation of the regioselective product **6** was confirmed *via* authentic reaction of 4-benzyl-phthalazin-1-ol, which was allowed to react with 1,3-dichloro-propan-2-ol to afford *O*-(3-chloro-2-hydroxypropyl) phthalazine **5** furnished as major product in addition to epoxide derivative **6** through the proposal mechanism outlined in (Scheme 5). *O*-Alkyl-phthalazine derivative **5** was ascertained from its spectral data, where its IR spectrum revealed bands in the region of 3397–3345 cm^{-1} attributable to υOH. Herein, we reported the designing and synthesis of biological active phthalazinone analogues with unique differences in the aglycone moieties.

Scheme 4. Synthesis route for compounds **5** and **6**.

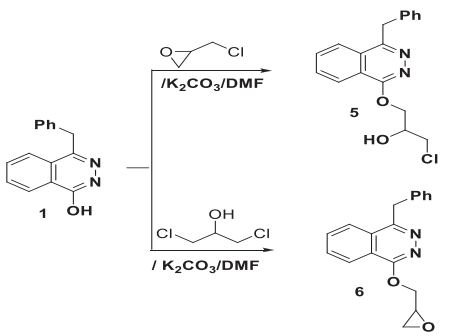

This new approach for synthesis of potent phthalazinone analogue pertains to modified nucleobases that are of neither the purine nor pyrimidine types. 4-Benzylphthalazine-1-ol **1** was subjected to react with (2-acetoxyethoxy)methyl bromide and 4-bromo butyl acetate with anhydrous K_2CO_3/DMF to afford the corresponding *N*-cyclo-nucleosides **7** and **8**, respectively (Scheme 6).

Structures of compounds **7** and **8** were ascertained from the spectroscopic and elemental analyses data. IR spectra exhibited two carbonyl groups for acetoxy groups that agreed well with the proposed structures. Treatment of acyclic-nucleosides **7** and **8** with CH_3OH/TEA and little drops of water resulted to deacetylation of acyclic-nucleosides afforded the free acyclo-nucleosides **9** and **10** in 75% yields. Assignments of **9** and **10** structures were elaborated by their spectral data IR, ^{1}H-NMR, and elemental analysis where it was expedient with the

Scheme 5. The proposal mechanism for the formation of compound **6**.

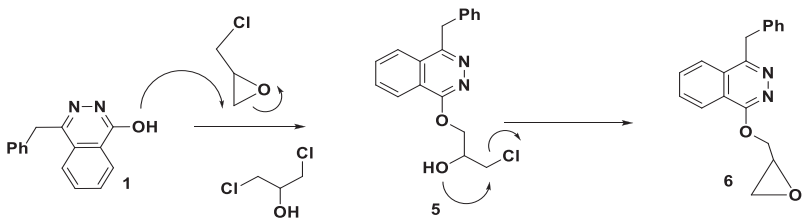

Scheme 6. Synthesis route for compounds **7–10**.

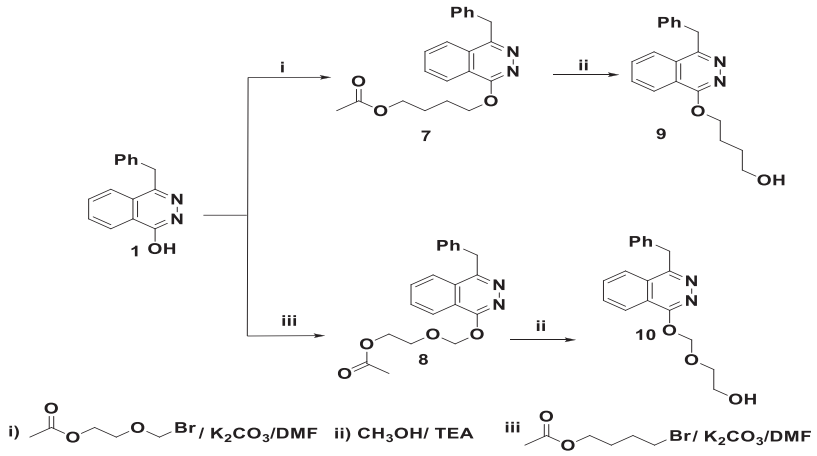

predicted structures. The IR spectra of **9** and **10** exhibited the presence of stretching absorption bands in the region 3445–3460 cm^{-1} revealed the presence of a free hydroxyl group moreover, the absence of a gathering band of acetoxy carbonyl groups. Furthermore, the reaction of the phthalazine **1** with chloroacetic hydrazide as alkyl halide took place *via* SN^2 reaction afforded the corresponding phthalazine hydrazide **11**. Reaction of the hydrazide **11** with different carbon electrophiles, for example, aromatic aldehydes, ethyl acetoacetate, and phthalic anhydride, afforded arylidene **12**, pyrazole **13**, and isoindolin-1,3-dione **14**, respectively (Scheme 7).

In contrast, refluxing of compound **1** with different aldehydes, namely, benzaldehyde, *p*-chlorobenzaldehyde, and *p*-methoxybenzaldehyde, pyrazolidine and 3-sulfonic acid-1-imidazolopyridinium hydrogen sulfate, $[Simp]HSO_4$ as a catalyst it afforded: 4-(4-(benyzl)-1-oxophthalazin-1-yl)(aryl)methyl)pyrazolidine-3,5-dione (**15**) (Scheme 8). The structures of compounds **15a–c** were elucidated from correct spectral data. The IR spectrum exhibited the presence of strong stretching absorption bands at regions 1623, 1670, and 3381 due to *v*CO and *v*NH, respectively.

The antimicrobial studies. All the synthesized compounds were examined to assess their growth inhibition potential against Gram-positive bacteria *Staphylococcus aureus* ATCC 06538, Gram-negative bacteria *Escherichia coli* ATCC 10536, pathogenic fungi *Candida albicans* ATCC 1023, and *Aspergillus flavus* using antimicrobial activity screening and evaluating agar diffusion assay. Peptidoglycan is a unique and essential component of the bacterial cell envelope. These muropeptides of bacterial cell envelop can be altered or modified by hydrolases *via* the action of bacterial

Scheme 7. Synthesis route for compounds **11–14**.

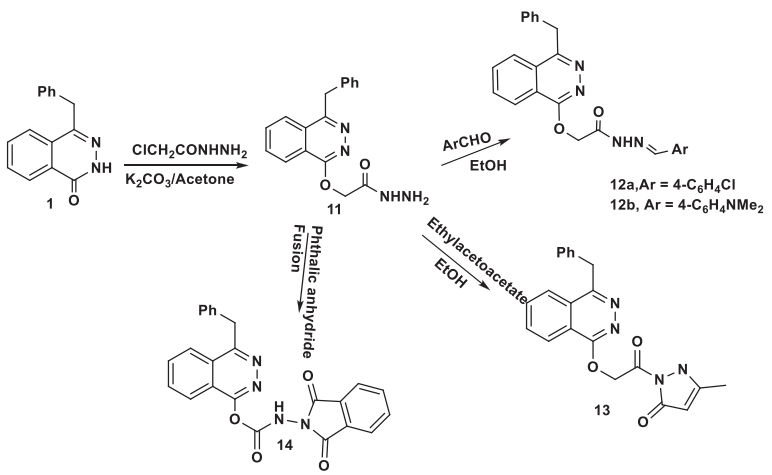

Scheme 8. Synthesis route for compounds **15a–c**.

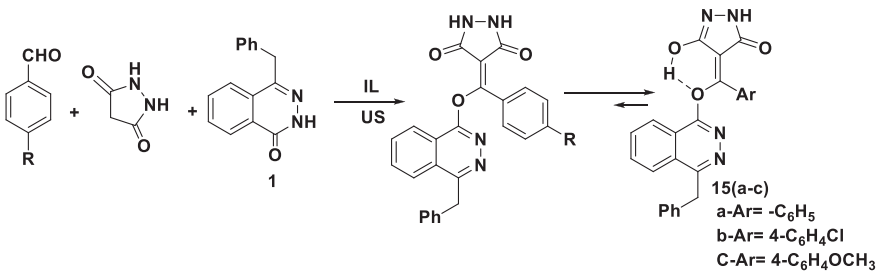

glycolytic and peptidolytic enzymes. In some pathogenic bacteria, for example, *Streptococcus pneumonia* and *Listeriamono cytogenes* [39,40] are also conventional for bacteria to deacetylate *N*-acetyl glucosamine residues. Meanwhile, a moderate activity was observed against *E. coli*, *S. aureus*, and *C. albicans* for compounds that have activity towards it. Most compounds from **1** to **15** were observed to possess the greatest antimicrobial activity. *Ampicillin*, *Streptomycin*, and *Nystatin* were used as positive control. Minimum inhibitory and microbicidal concentration (MIC) was determined for each of the active compounds along with positive control. No activity was detected for all the synthesized compounds towards *A. flavus*. The following Tables 1 and 2 showed the results of antimicrobial activity and MICs for the most potent compounds. *O*-Alkyl-phthalazine compounds chiefly phthalazine bearing epoxide, hydrazide, arylidene, and pyrazoline showed very influential *in vitro* activity against both susceptible and multidrug-resistant isolates of *Mycobacterium tuberculosis*. Optimization of the scaffold proceeds with the goal of lessening toxicity while maintaining potency. These compounds represent a promising new scaffold for the treatment of drug-resistant bacterial pathogens.

Density functional theory-based characterization. From the MIC of the most potent *O*-alkyl-phthalazine compounds **6**, **11**, **12a**, and **15b**, the quantum mechanical program was used for the molecular parameters for the most potent compounds listed in Table 3 and the fully optimized minimum energy geometrical configuration of the most potent antimicrobial compounds (see more in the supporting information). Proceeds, density functional theory-based MIC of such compounds supported their high antimicrobial activity.

Table 1

Antimicrobial efficacy of compounds **1** to **15**.

Synthesized compounds	*Staphylococcus aureus*	*Escherichia coli*	*Aspergillus niger*	*Candida albicans*
1	17	22	21	16
2	18	20	21	15
3	19	23	22	16
4	17	20	21	14
5	20	19	20	21
6	17	18	21	20
7	28	22	18	15
8	21	19	17	14
9	22	18	16	16
10	20	17	18	16
11	15	17	21	12
12a	13	12	17	11
12b	12	16	18	10
13	14	13	0.0	11
14	16	16	19	13
15a	15	14	13	12
15b	16	22	18	15
15c	20	21	19	16
Ampicillin	0.0	22	0.0	0.0
Streptomycin	20	21	0.0	0.0
Nystatin	0.0	0.0	0.0	22

Zone of inhibition diameter measured in mm. No activity (0.0), inhibition zone (<7 mm), weak activity (7–10 mm), moderate activity (11–15 mm), strong activity (>15 mm), solvent $CDCl_3$ (6 mm).

Table 2

Minimum inhibitory concentration values for the most potent compounds (μg/mL).

Compounds	Gram-positive bacteria	Gram-negative bacteria	Fungi	
	Staphylococcus aureus	*Escherichia coli*	*Candida albicans*	*Aspergillus niger*
6	12.5	12.5	25	50
11	12.5	12.5	25	50
12a	12.5	25	25	50
15b	12.5	25	25	50

Table 3

Quantum chemical parameters calculated for the studied compounds.

Compounds	E_{HOMO} (eV)	E_{LUMO} (eV)	ΔE (eV)	I (eV)	A (eV)	χ (eV)	η (eV)	ΔN	μ (Debye)	A_{molec} (squared Å)
6	−8.572	−5.524	3.011	9.095	0.384	4.740	4.356	0.259	8.790	297.443
11	−8.130	−5.525	2.591	8.883	0.832	4.858	4.026	0.266	9.558	312.608
12a	−5.537	−5.207	0.330	8.661	0.657	4.659	4.002	0.292	12.139	590.401
15b	−3.475	−2.724	0.751	8.135	1.239	4.687	3.448	0.335	16.395	619.866

It is well known that high E_{HOMO} are likely to indicate a strong tendency of the molecule to donate electrons. The low values of the energy gap ($\Delta E = E_{LUMO} - E_{HOMO}$) will render good inhibition efficiencies, because the energy needed to remove an electron from the last occupied orbital will be low [41–43]. The ΔE of a molecule is a measure of the hardness or softness of a molecule. Hard molecules are characterized by larger values of ΔE and vice versa. The linear correlation between E_{HOMO} energy level and the antimicrobial activity proved that the lower the HOMO energy (more negative values) of the *O*-alkyl-phthalazine, the greater the trend of accepting electrons. The order of decreasing E_{HOMO}, increasing E_{LUMO} values, and the energy gap (ΔE) is directly proportional with increasing the antimicrobial efficiency. The tendency of an electron cloud to be distorted from its normal shape is referred to as its polarizability: the greater the polarizability the more inhibitor molecules will leave from solvent bulk to be absorbed by radical or oxidized surface to form a protective film; we can consider the polarizability as a resultant of all intramolecular electron transfer interactions. This increased volume enhances the ease of the distortion of the electron cloud, which will promote the adsorption of the phthalazine.

Density functional theory can provide visions into the electronic and structural characteristics of heterocyclic compounds [42]. In this, the parameters of density functional study achieved for phthalazin-1-ol derivatives as considered Frontier molecular orbital energies (FMO). HOMO energies are considered as nucleophiles, while the LUMO characterize the electrophilic sites [43]. High-occupied molecular orbital energies E_{HOMOs} be present a parameter of ionization potential and their states value of the heterocyclic susceptibility be reacted with electrophiles, whereas the LUMO energies (E_{LUMOs}) bring up the electron affinity and become towards a nucleophiles. To find these parameters, phthalazin-1-ol must be optimized geometrically first then HOMO and LUMO distributed cf. Figure 1 in which HOMOs are concentrated over the phthalazine unit, while LUMOs are focused on the pyridazine moiety. This is general for thephthalazin-1(2H)-one, phthalazin-1-ol and O-alkylphthalazine that are outlined in Figure 1.

Consequently, *O*-alkyl-phthalazine moieties are the most active centers in the study for electron transfer (either electron donation or acceptance). The obtained E_{HOMO} and E_{LUMO} of the synthesized compounds are listed in Table 2. The listed results indicate that the values of gap energy (ΔE), where $\Delta E = E_{LUMO} - E_{HOMO}$, follow the order: arylidene **12a** < pyrazolidine **15b** < hydrazide **11** < epoxide **6**. ΔE is indicative for the reactivity of phthalazin-1-ol having small $E_{LU} - E_{HO}$ values are mostly mentioned to as soft molecules, whereas large values the so-called hard compounds. Generally, the soft molecules are more penetrate to the antimicrobial surface because of definitely donating electrons by heteroatoms rich non-bonded electrons to positive charge of the microbe surface [42]. Moreover, the phthalazine moiety stayed nucleophilic center because of transferring electron to the microbial cell wall during operating conditions. Low ΔE of the synthesized *O*-alkyl-phthalazine provided good interaction with aglycone of cell wall of bacteria. This is due to the binding energy of the phthalazine-aglycone reduce an electron density from (HOMO) of the phthalazine nuclus. So the *O*-alkyl-phthalazine can definite polarizable more than hard compounds that help to expect the molecular parameter of for instance electron

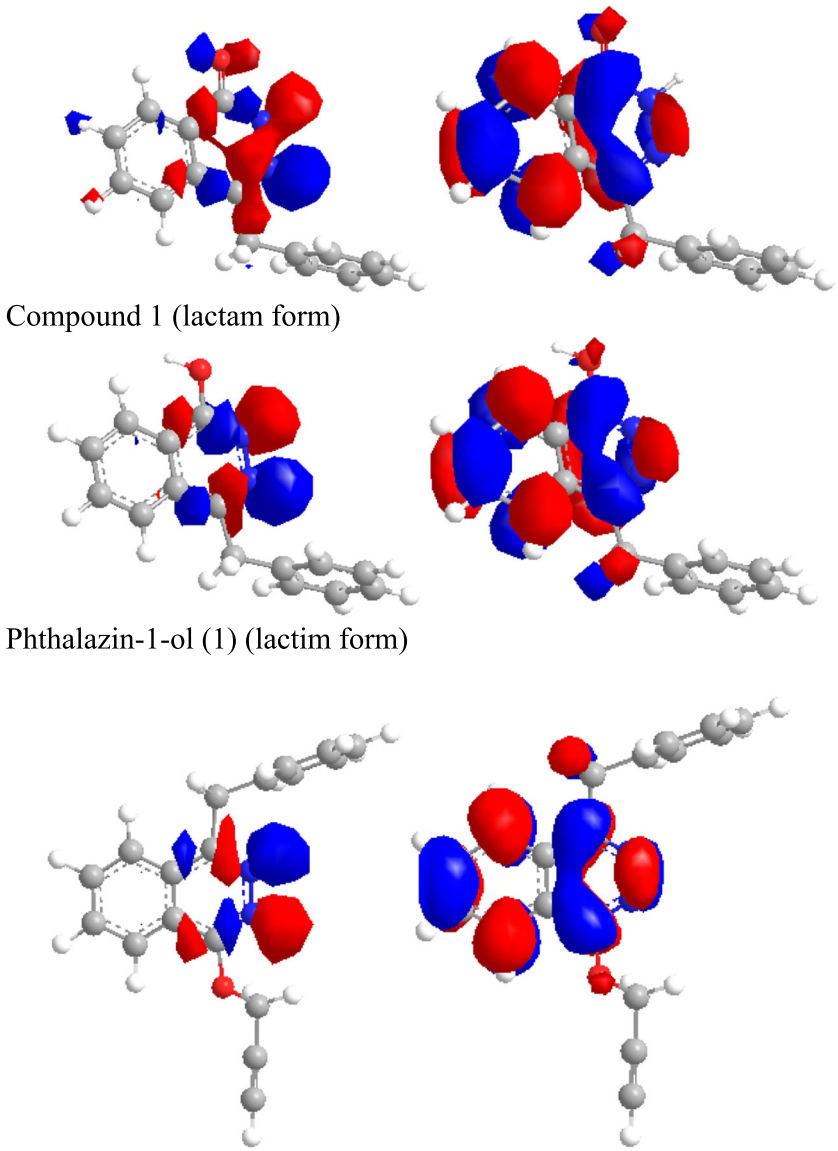

Figure 1. The electronic structures HOMO at left and LUMO at right for the phthalazin-1(2*H*)-one, phthalazin-1-ol, and *O*-alkyl-phthalazine: compound **1** (lactam form); phthalazin-1-ol (**1**) (lactim form). [Color figure can be viewed at wileyonlinelibrary.com]

affinity ($A = -E_{LUMO}$), ionization potential ($I = -E_{HOMO}$), chemical hardness ($\eta = I - A/2$), and electronegativity ($\chi = I + A/2$), affording epoxide **6** < hydrazide **11** < pyrazoline **15b** < arylidene **12a** [43].

For the synthesized phthalazine, χ, η, and chemical softness ($s = 1/\eta$) became 6 eV for the arylidene **12a** that is lower than aglycone of bacteria. Thus, aglycone–phthalazine interaction may proceed *via* electron transfer for the reason that electrophilicity index $\omega = E^2/\eta$ of glycone (good electrophile type has a high (E) value and a low (η) value). Therefore, the arylidene **12a** and pyrazoline **15b** have a high nucleophilicity index ($\Delta N_{max} = E/\eta$) and are predicted to be the best powerful additive for antimicrobial cell [44].

CONCLUSION

An efficient green synthetic route for preparation for *O*-alkyl-phthalazine derivatives that contain arylidene, pyrazoline, hydrazides, and oxirane moieties was prepared and characterized spectroscopically. The most potent antimicrobial compounds are the newly synthesized phthalazine derivatives **6**, **11**, **12a**, and **15b**. The studies have revealed that density functional theory-based MIC of such compounds that have hydrophobic and electrophilic groups supports the high antimicrobial activities of the *O*-alkyl-phthalazine containing epoxide, hydrazide, arylidene, and pyrazoline precursors. Based on the aforementioned studies, the promising compounds

can be submitted to *in vivo* antimicrobial studies as a future perspective.

EXPERIMENTAL

All chemicals and reagents were purchased from the Aldrich Chemical Co. Melting points are uncorrected and were measured on a Gallen Kamp electric melting point apparatus. -IR spectra were run and recorded on a pye-Unicam SP-3-300, Shimadzu FTIR 8101 PC infrared spectrophotometers, and ultrasound device (600 W, Italy) at the Faculty of Science, Ain Shams University.

The ^{1}H-NMR spectra were recorded on a Varian Mercury VX-300 MHz and ^{13}C-NMR (125 MHz) using tetramethylsilane as internal standard in deuterated dimethylsulfoxide (DMSO-d_6). Chemical shifts are measured in (δ) ppm. The mass spectra were recorded on a Shimadzu GCMS-QP-1000EX mass spectrometer at 70 e. Elemental analyses were carried out at the microanalytical center of Ain Shams University. All the reactions and the purity of the new compounds were followed and cheeked by thin-layer chromatography (TLC) using TLC aluminum sheets silica gel.

4-Benzylphthalazin-1-ol (1). Phthalic anhydride (0.01 mol), phenylacetic acid (0.01 mol), and hydrazine hydrate (0.015 mol, 0.75 mL) were grinded together in a mortar. After that, the reaction mixture was then transferred into a 100-mL round bottom flask, and (5 mL) ethanol was then added. The reaction was monitored when placed in the maximum energy area in an ultrasonic cleaner bath. The bath temperature was controlled by addition or removal of water at 30°C. The reaction progress was monitored by TLC using $CHCl_3$: EtOAc *v*/v 50:50 until the starting reactants disappeared as indicated by TLC. Within 20–25 min of irradiation, a white crystal product was obtained. A beaker with crushed ice was prepared, and then the solid mixture was poured into it with continuous stirring; a white solid product was obtained that was dried and recrystallized from acetic acid.

Yield (93%), mp 182–184°C. IR (KBr, cm^{-1}): υ3438 (OH). ^{1}H-NMR (300 MHz, DMSO-d_6) δppm: 12.72 (br. s, 1H, OH, D_2O) was heated under sonication for 40 min. The solvent was evaporated, and exchangeable, 7.62–8.35 (m, 9H, Ar H), 3.39 (s, 2H, CH_2). MS, m/z (%): 236 [M$^{\cdot+}$] (100.0%). ^{13}C-NMR (125 MHz, DMSO-d_6): 178.7, 149.7, 141.2, 132.2, 131.9 (2), 130.1 (2), 129.2 (2), 128.4, 127.8, 126.4, 120.1, 39.8. *Anal*. Calc. for $C_{15}H_{12}N_2O$ (236): % C, 76.27; H, 5.12; N, 11.86; Found: C, 76.42; H, 4.95; N, 11.54.

General procedure for preparation of compounds 2 and 3. A solution of the proper alkyl halide, namely, propargyl bromide or allyl bromide (0.01 mol), compound **1** (0.01 mol), and anhydrous K_2CO_3 (0.01 mol) in dry acetone (15 mL), the residue was washed with cold water, filtered off, dried, and recrystallized from ethanol.

1-Benzyl-4-(prop-2-yn-1-yloxy)phthalazine (2). Yield (88%), mp 159–160°C. IR (KBr, cm^{-1}): υ3248, δ 638 (C–H) alkynyl. ^{1}H-NMR (300 MHz, DMSO-d_6) δppm: 8.36–7.35 (m, 9H, ArH), 4.97 (s, 2H, OCH_2), 3.41 (s, 2H, CH_2), 2.91 (s, 1H, acetylenic proton). MS, m/z (%): 274 [M$^{\cdot+}$] (100.0%). ^{13}C-NMR (125 MHz, DMSO-d_6): 178.7, 144.9, 134.7, 132.2, 131.9, 130.1, 129.2 (2), 128.4 (2), 127.5, 126.5, 125.4, 119.5, 78.2, 72.1, 50.9, 39.3. *Anal*. Calc. for $C_{18}H_{14}N_2O$ (274): % C, 78.81; H, 5.14; N, 10.21; Found: C, 78.42; H, 4.95; N, 10.25.

1-(Allyloxy)-4-benzylphthalazine (3). Yield (82%), mp 125–126°C. IR (KBr, cm^{-1}): ν3127 (C–H) alkenyl. ^{1}H-NMR (300 MHz, DMSO-d_6) δppm: 8.34–7.53 (m, 9H, ArH), 5.96 (m, 1H, CH_2–C<u>H</u>=CH_2), 5.64–5.14 (2dd, 2H, CH=C<u>H</u>$_2$, J = 15.8, 12.6, 5.4 Hz), 4.28 (d, 2H, OCH_2). MS, m/z (%): 276 [M$^{\cdot+}$] (100.0%). ^{13}C-NMR (125 MHz, DMSO-d_6): δ 178.7, 143.9, 133.4, 132.2, 131.5, 130.9 (2), 129.2 (2), 128.4 (2), 127.5, 126.5, 125.4, 123.5, 117.4, 75.8, 39.3. *Anal*. Calc. for $C_{18}H_{16}N_2O$ (276): % C, 78.24; H, 5.84; N, 10.14; Found: C, 77.97; H, 5.67; N, 10.48.

1-Benzyl-4-(2,3-dibromopropoxy) phthalazine (4). A solution of **3** (0.01 mol) in carbon tetrachloride (20 mL) and bromine (0.015 mol) in carbon tetrachloride (20 mL) was added and stirred for 30 min at room temperature, and then stirring was continued for 3 h. The solid product formed was filtered off, dried, and crystallized from ethanol.

Yield (80%), mp 140–142°C. IR (KBr, cm^{-1}): ν2961 (C–H), 648 (C–Br). ^{1}H-NMR (300 MHz, DMSO-d_6) δppm: 8.40–7.31 (m, 9H, ArH), 4.91–4.83 (m, 1H, CH_2<u>C</u>HBrCH_2Br), 4.60–4.54 (d, 2H, CH_2Br, J = 8.2 Hz), 4.08 (d, 2H, OCH_2, J = 7.7 Hz), 2.41 (s, 2H, CH_2Ph). MS, m/z (%): 438 [M$^{\cdot+}$+2] (49.0%), 436 [M$^{\cdot+}$] (100.0%), 434 [M$^{\cdot+}$-2] (51.0%). *Anal*. Calc. for $C_{18}H_{16}Br_2N_2O$ (436): % C, 49.57; H, 3.70; N, 6.42; Found: C, 49.17; H, 3.72; N, 6.48.

***O*-Alkyl-phthalazine (5) and (6).** 4-Benzyl-phthalazin-1-ol **1** (0.01 mol), epichlorohydrin, and/or 1,3-dichloropropanol (0.01 mol) in anhydrous K_2CO_3 (0.01 mol)/dry DMF (30 mL) were mixed together and then sonicated for 1 h in a bath-type sonicator. The mixture was filtered off under reduced pressure to remove the excess solvent, and the residue was diluted with water. The solid product formed was recrystallized from ethanol.

1-((4-Benzylphthalazin-1-yl)oxy)-3-chloropropan-2-ol (5). Yield (36%), mp 122–123°C. IR (KBr, cm^{-1}): ν3445 (OH), 772 (C–Cl). ^{1}H-NMR (300 MHz, DMSO-d_6) δppm: 8.34–7.33 (m, 9H, ArH), 4.83 (s, 1H, OH, exchangeable with D_2O), 4.62 (m, 1H, C<u>H</u>OH), 4.27–4.16 (m, 2H, methylene protons of CH_2Cl), 3.45 (m, 2H, NCH_2), 2.39 (s, 3H, CH_3). MS, m/z (%): 328 [M$^{\cdot+}$] (100.0%). ^{13}C-NMR

(125 MHz, DMSO-d_6): δ 158.4, 138.6, 134.7, 132.9, 132.3, 131.5, 131.0, 130.4, 129.2, 128.2, 127.5, 126.2, 123.3, 71.2, 55.4, 48.4, 19.2. *Anal*. Calc. for $C_{18}H_{17}ClN_2O_2$ (328): % C, 65.85; H, 5.21; N, 8.52; Found: C, 65.70; H, 5.27; N, 8.35.

1-Benzyl-4-(oxiran-2-ylmethoxy) phthalazine (6). Yield (54%), mp 124–126°C. IR (KBr, cm^{-1}): ν1245, 930 and 830 (C–O epoxide). ^{1}H-NMR (300 MHz, DMSO-d_6) δppm: 8.43–7.48 (m, 9H, ArH), 4.68–4.42 (dd, 2H, OCH_2, J = 5.52), 4.32–4.25 (m, 1H proton of oxirane ring), 4.15–4.05 (2dd, 2H, CH_2 of oxirane ring; J = 14.2, 11.8 Hz), 2.38 (s, 2H, Ph$\underline{CH_2}$). MS, m/z (%): 292 [$M^{\cdot+}$] (100.0%). ^{13}C-NMR (125 MHz, DMSO-d_6): δ 158.4, 138.9, 134.7, 132.9, 132.3, 131.5, 131.0, 130.4, 129.2 (2), 128.2, 127.5, 126.2, 123.3, 55.4, 47.4, 43.1, 19.2. *Anal*. Calc. for $C_{18}H_{16}N_2O_2$ (292): % C, 73.95; H, 5.52; N, 9.58; Found: C, 73.71; H, 5.37; N, 9.65.

Compounds 7 and 8. A mixture of **1** (0.01 mol), 4-bromobutylacetate, and/or 2-(bromomethoxy)ethylacetate (0.01 mol) in anhydrous K_2CO_3 (0.01 mol)/dry DMF (30 mL) was stirred ultrasonically at room temperature for 1 h, then evaporated the excess solvent under reduced pressure, and then diluted with water. The solid obtained was recrystallized from ethanol.

4-((4-Benzylphthalazin-1-yl)oxy)butyl acetate (7). Yield (61%), mp 90–92°C. IR (KBr, cm^{-1}): *ν*1737 (CO ester), 1256 (C–O ether). ^{1}H-NMR (300 MHz, DMSO-d_6) δppm: 8.38–7.66 (m, 9H, ArH), 3.84 (t, 2H, CH_2OCO, J = 6.6 Hz), 3.45 (t, 2H, OCH_2, J = 6.9 Hz), 2.36 (s, 2H, $PhCH_2$), 2.20 (s, 3H, CH_3CO), 1.93–1.89 (m, 4H, $2CH_2$). MS, m/z (%): 352 [$M^{\cdot+}$] (100.0%). ^{13}C-NMR (125 MHz, DMSO-d_6): δ 170.0, 158.4, 138.2, 134.7, 132.9, 132.3, 131.5, 131.0, 130.4, 129.2 (2), 128.2, 127.5, 126.2, 123.3, 87.4, 66.1, 63.7, 50.5, 39.1, 33.2. *Anal*. Calc. for $C_{21}H_{22}N_2O_3$ (350): % C, 71.98; H, 6.33; N, 7.99; Found: C, 71.89; H, 6.29; N, 7.90.

2-(((4-Benzylphthalazin-1-yl)oxy)methoxy)ethylacetate (8). Yield (98%), mp 92–94°C. IR (KBr, cm^{-1}): *ν*1731 (CO ester), 1252 (C–O ether). ^{1}H-NMR (300 MHz, DMSO-d_6) δppm: 8.38–7.69 (m, 9H, ArH), 4.92 (s, 2H, OCH_2O), 4.21–4.03 (m, 4H, $2OCH_2$), 2.38 (s, 2H, $PhCH_2$), 1.96 (s, 3H, CH_3CO). MS, m/z (%): 350 [$M^{\cdot+}$] (100.0%). ^{13}C-NMR (125 MHz, DMSO-d_6): δ 170.0, 158.4, 138.1, 134.7, 132.9, 132.3, 131.5, 131.0, 130.4, 129.2 (2), 128.2, 127.5, 126.2, 123.3, 64.1, 56.7, 41.7, 40.5, 38.2. *Anal*. Calc. for $C_{20}H_{20}N_2O_4$ (352): % C, 68.17; H, 5.72; N, 7.95; Found: C, 65.20; H, 5.63; N, 7.81.

Compounds 9 and 10. A mixture of **7** and/or **8** (0.01 mol), triethylamine (1 mL), and few drops of water in methanol (30 mL) was stirred at room temperature for 1 h and then left overnight. The excess solvent was evaporated under reduced pressure, and the formed residue was recrystallized from ethanol.

4-((4-Benzylphthalazin-1-yl)oxy)butan-1-ol (9). Yield (75%), mp 114–115°C. IR (KBr, cm^{-1}): *ν*3445 (OH), 1252 (C–O ether). ^{1}H-NMR (300 MHz, DMSO-d_6) δppm: 8.38–7.35 (m, 9H, ArH), 4.41 (bs, 1H, J = 5.2, OH, exchangeable with D_2O), 4.16 (t, 2H, CH_2O, J = 6.6), 3.41 (t, 2H, NCH_2, J = 6.6 Hz), 2.10 (s, 2H, $PhCH_2$), 1.79 (m, 2H, CH_2), 1.45 (m, 2H, CH_2). MS, m/z (%): 310 [$M^{\cdot+}$] (100.0%). ^{13}C-NMR (125 MHz, DMSO-d_6): δ 170.0, 158.4, 141.1, 137.7, 132.9, 132.3, 131.5, 131.0, 130.4, 129.2 (2), 128.2, 127.5, 126.2, 123.3, 64.1, 56.7, 41.7. *Anal*. Calc. for $C_{19}H_{20}N_2O_2$ (308): % C, 74.00; H, 6.54; N, 9.08; Found: C, 74.12; H, 6.59; N 9.38.

2-(((4-Benzylphthalazin-1-yl)oxy)methoxy)ethan-1-ol (10). Yield (75%), mp 121–123°C. IR (KBr, cm^{-1}): *ν*3465 (OH), 1261 (C–O ether). ^{1}H-NMR (300 MHz, DMSO-d_6) δppm: 8.53–7.63 (m, 9H, ArH), 4.89 (t, 1H, OH, J = 6.9 Hz, exchangeable in D_2O), 5.34 (s, 2H, CH_2O), 3.52 (t, 2H, CH_2OCO, J = 5.5 Hz), 3.34 (t, 2H, OCH_2, J = 5.5 Hz), 2.23 (s, 2H, $PhCH_2$). MS, m/z (%): 308 ($M^{\cdot+}$, 100.0%). ^{13}C-NMR (125 MHz, DMSO-d_6): δ 168.2, 154.4, 138.1, 134.7, 132.9, 132.3, 131.5, 130.4, 129.2 (2), 128.2, 127.5, 126.2, 123.3, 64.1, 56.7, 41.7, 40.5, 38.2. *Anal*. Calc. for $C_{18}H_{18}N_2O_3$ (310): % C, 69.66; H, 5.85; N, 9.03; Found: C, 69.70; H, 5.73; N 9.10.

2-((4-Benzylphthalazin-1-yl)oxy)acetohydrazide (11). A mixture of **1** (0.01 mol), 2-chloroacetic acid hydrazide (0.01 mol), and anhydrous K_2CO_3 (0.01 mol) in dry DMF (30 mL) was stirred ultrasonically at room temperature for 1 h. The excess solvent was evaporated under reduced pressure, and the reaction mixture was diluted with water. The solid obtained was recrystallized from ethanol.

Yield (75%), mp 154–156°C. IR (KBr, cm^{-1}): *ν*3378, 3267, 3159 (NH), 2956 (CH), 1252 (C–O ether). ^{1}H-NMR (300 MHz, DMSO-d_6) δppm: 11.34 (bs, 1H, NH, J = 8.3 Hz, exchangeable in D_2O), 8.53–7.63 (m, 9H, ArH), 5.52 (bs, 2H, NH_2, J = 5.5 Hz), 5.34 (s, 2H, OCH_2), 2.43 (s, 2H, $PhCH_2$). MS, m/z (%): 308 [$M^{\cdot+}$] (100.0%). *Anal*. Calc. for $C_{17}H_{16}N_4O_2$ (308): % C, 66.22; H, 5.23; N, 18.17; Found: C, 66.18; H, 5.28; N, 18.20.

Compounds 12a and 12b. A mixture of **11** (0.01 mol) and aromatic aldehydes, namely, 4-chlorobenzaldehyde and *N*,*N*-dimethyl benzaldehyde (0.01 mol), in boiling ethanol (30 mL) was stirred ultrasonically at 60°C for 1 h. The excess solvent was evaporated under reduced pressure, and the reaction mixture was diluted with water. The solid obtained was recrystallized from ethanol.

2-((4-Benzylphthalazin-1-yl) oxy)-N'-(4-chlorobenzylidene) acetohydrazide (12a). Yield (75%), mp 138–140°C. IR (KBr, cm^{-1}): *ν*3313 (NH), 3064, 2956 (CH), 1252 (C–O ether). ^{1}H-NMR (300 MHz, DMSO-d_6) δppm: 11.17 (bs, 1H, NH, J = 8.1 Hz, exchangeable in D_2O), 8.43–7.28 (m, 13H, ArH), 9.52 (s, 1H, CH), 5.34 (s, 2H, OCH_2), 2.43 (s, 2H, $PhCH_2$). MS, m/z (%): 432 [$M^{\cdot+}$+2] (15.0%), 430 [$M^{\cdot+}$] (100.0%). *Anal*. Calc. for $C_{24}H_{19}ClN_4O_2$ (430): % C, 66.90; H, 4.44; Cl, 8.23; N, 13.00; Found: C, 66.88; H, 4.49; Cl, 8.29; N, 13.06.

2-((4-Benzylphthalazin-1-yl) oxy)-N'-(4-(dimethylamino) benzylidene)acetohydrazide (12b). Yield (75%), mp 142–144°C. IR (KBr, cm^{-1}): *v*3289 (NH), 3052, 2987 (CH), 1252 (C–O ether). ^{1}H-NMR (300 MHz, DMSO-d_6) δppm: 11.03 (bs, 1H, NH, *J* = 8.1 Hz, exchangeable in D_2O), 8.32–7.04 (m, 13H, ArH), 10.14 (s, 1H, CH), 5.19 (s, 2H, OCH_2), 3.12 (s, 6H, $(CH_3)_2N$), 2.51 (s, 2H, $PhCH_2$). MS, m/z (%): 439 [$M^{\cdot+}$] (100.0%). *Anal*. Calc. for $C_{26}H_{25}N_5O_2$ (439): % C, 71.05; H, 5.73; N, 15.93; Found: C, 71.1; H, 5.68; Cl, 8.29; N, 15.89.

2-(2-((4-Benzylphthalazin-1-yl)oxy)acetyl)-5-methyl-1,2-dihydro-3H-pyrazol-3-on (13). A mixture of **11** (0.01 mol) and ethyl acetoacetate (0.01 mol) in boiling ethanol (30 mL) was stirred ultrasonically at 40°C for 30 min. The excess solvent was evaporated under reduced pressure. The solid obtained was recrystallized from ethanol.

Yield (80%), mp 192–194°C. IR (KBr, cm^{-1}): *v*3313 (NH), 3064, 2956 (CH), 1252 (C–O ether). ^{1}H-NMR (300 MHz, DMSO-d_6) δppm: 8.43–7.28 (m, 10H, ArH, 1H of pyrazolone), 5.28 (s, 2H, OCH_2), 2.85 (s, 3H, CH_3-Pyraz), 2.43 (s, 2H, $PhCH_2$). MS, m/z (%): 432 [$M^{\cdot+}$+2] (15.0%), 374 [$M^{\cdot+}$] (100.0%). *Anal*. Calc. for $C_{21}H_{18}N_4O_3$ (374): % C, 67.37; H, 4.85; N, 14.96; Found: C, 67.40; H, 4.82; N, 14.98.

4-Benzylphthalazin-1-yl(1,3-dioxoisoindolin-2-yl)carbamate (14). A grind mixture of **11** (0.01 mol) and phthalic anhydride (0.01 mol) in dry ethanol (5 mL) was stirred ultrasonically at 90°C for 1 h. The excess solvent was evaporated under reduced pressure, and the reaction mixture was diluted with water. The solid obtained was recrystallized from ethanol.

Yield (75%), mp 206–208°C. IR (KBr, cm^{-1}): *v*3219 (NH), 3058 (CH), 1252 (C–O ether). ^{1}H-NMR (300 MHz, DMSO-d_6) δppm: 12.02 (bs, 1H, NH, exchangeable in D_2O), 8.53–7.63 (m, 13H, ArH), 5.34 (s, 2H, OCH_2), 2.43 (s, 2H, $PhCH_2$). MS, m/z(%): 308 [$M^{\cdot+}$] (100.0%). *Anal*. Calc. for $C_{24}H_{16}N_4O_4$ (424): % C, 67.92; H, 3.80; N, 13.20; Found: C, 67.78; H, 3.64; N, 13.00.

Compounds 15a, **15b**, **and 15c**. A mixture of pyrazolidine-3,5-dione (0.01 mol), phthalazine **1** (0.01 mol), and aldehyde, namely, benzaldehyde, 4-chlorobenzaldehyde, and 4-methoxybenzaldehyde (0.04 mmol), with [simp]HSO_4 (0.4 mmol) in ethanol (30 mL) was heated at 100°C for 6 h. After cooling, the residue was recrystallized from ethanol.

(4-(Benzyl)-1-oxophthalazin-2(1H)-yl)(phenyl)methyl) pyrazolidine-3,5-dione (15a). Yield (80%), mp 112–114°C. IR (KBr, cm^{-1}): *v*3452 (OH), 3342 (NH), 1652 (COpyraz). ^{1}H-NMR (300 MHz, DMSO-d_6) δppm: 12.36 (s, 1H, NH exchangeable with D_2O), 9.64 (s, 1H, OH exchangeable with D_2O), 8.23–7.46 (m, 14H, ArH), 2.52 (s, 2H, $PhCH_2$). MS, m/z (%): 422 [$M^{\cdot+}$] (100.0%). ^{13}C-NMR (125 MHz, DMSO-d_6): δ 176.5, 159.4, 134.6, 132.6, 132.3, 131.5, 131.0, 130.4, 129.2, 128.2, 127.5, 126.0, 123.3, 95.5, 76.2, 70.0, 69.3, 64.6, 52.8, 38.4. *Anal*. Calc. for $C_{25}H_{18}N_4O_3$ (422): % C, 71.08; H, 4.30; N, 13.26; Found: C, 70.84; H, 4.17; N, 13.00.

4-(4-Chlorophenyl)(4-(benzyl)-1-oxophthalazin-2(1H)yl) methyl)pyrazolidine-3,5-dione (15b). Yield (80%), mp 132–134°C. IR (KBr, cm^{-1}): *v*3390 (OH), 3287 (NH), 1657 (COpyraz). ^{1}H-NMR (300 MHz, DMSO-d_6) δppm: 12.25 (s, 1H, NH exchangeable with D_2O), 9.64 (s, 1H, OH exchangeable with D_2O), 8.23–7.46 (m, 13H, ArH), 2.51 (s, 2H, $PhCH_2$). MS, m/z (%): 458 [$M^{\cdot+}$+2] (30.0%). 456 [$M^{\cdot+}$] (100.0%). ^{13}C-NMR (125 MHz, DMSO-d_6): δ 178.2, 159.4, 134.6, 132.6, 132.3, 131.5, 131.0, 130.4, 129.2, 128.2, 127.5, 126.0, 123.3, 95.5, 76.2, 70.0, 69.3, 64.6, 52.3, 38.9. *Anal*. Calc. for $C_{25}H_{17}ClN_4O_3$ (456): % C, 65.72; H, 3.75; N, 12.26; Found: C, 65.54; H, 3.57; N, 12.00.

4-(4-(Benzyl)-1-oxophthalazin-2(1H)-yl)(4-methoxyphenyl) methyl)pyrazolidine-3,5-dione (15c). Yield (80%), mp 132–134°C. IR (KBr, cm^{-1}): *v*3402 (OH), 3293 (NH), 1655 (COpyraz). ^{1}H-NMR (300 MHz, DMSO-d_6) δppm: 12.25 (s, 1H, NH exchangeable with D_2O), 9.64 (s, 1H, OH exchangeable with D_2O), 8.23–7.46 (m, 13H, ArH), 3.82 (s, 3H, OCH_3), 2.51 (s, 2H, $PhCH_2$). MS, m/z (%): 452 [$M^{\cdot+}$] (100.0%). *Anal*. Calc. for $C_{26}H_{20}N_4O_4$ (452): % C, 69.02; H, 4.46; N, 12.38; Found: C, 68.83; H, 4.27; N, 12.13.

Screening for antimicrobial activity. In the screening process, four different strains of microorganisms were used *S. aureus* (Gram-positive), *E. coli* (Gram-negative), and antifungal screening against *Aspergillus niger* and *C. albicans*. The bacteria were grown in nutrient at 37°C and maintained on nutrient agar slants at 4°C, and fungal cultures were grown and maintained on potato dextrose agar slants at 4°C. It was collected from the Microbial Type Culture, from collection and Gene Bank (MTCC), Institute of Microbial Technology (IMTECH), Faculty of Science, Al-Azhar University. The antimicrobial activity assay was performed by both disc diffusions.

Antimicrobial evaluation. Antimicrobial activities of synthetic compounds were evaluated versus eight tested pathogenic strains using agar-well diffusion process. The strains of bacteria were grown up on nutrient agar medium (agar 15 gm, beef extract 3 gm, sodium chloride 5 gm, and peptone 5 gm, in 1-L distilled water) at 37°C for 18 h and were suspended in a saline solution (0.85% NaCl) and adjusted to a turbidity of 0.5 Mac Farland standards (108 CFU/mL); 90-mm diameter Petri plates were inoculated with the suspension. Wells with 6-mm diameter were punched in the agar and filled with the test samples to obtain different concentrations (viz. 15, 25, 35, 45, and 55 μL) of the extract. For antibacterial assay, *Ampicillin* and *Streptomycin* were used as a standard and *Nystatin* as antifungal assay. Plates were incubated at 37 ± 2°C for 24 h. Antimicrobial activities were

evaluated by measuring inhibition zone diameters, and the activity index was calculated for each of these. The experiments were conducted in triplicate. The same method was followed for testing antifungal activity using potato dextrose agar medium.

$$\text{Activity index} = \text{Inhibition zone of the sample} / \text{Inhibition zone of the standard}$$

Determination of minimum inhibitory concentration. Broth dilution method was used to determine the MIC of various extracts against tested microorganisms. For broth dilution, 1 mL of standardized suspension of a strain (106 CFU/mL) was added to each tube containing *O*-alkyl-phthalazine derivatives at various concentrations in nutrient broth medium. The tubes were incubated at 37°C for 24 h and 25°C for 48 h of bacteria fungal strains respectively observed for visible growth after straining them gently. MIC is reserved the lowest concentration of the extracts upon which there is turbidity after incubation. The highest dilution of a plant extract immobile retains an inhibitory effect against the growth of microorganisms.

Acknowledgments. We are thankful to the central laboratory of Faculty of Science, Ain Shams University, and its teamwork for all the facilities that have been provided in terms of the use of the available instruments used for the spectral analysis of the compounds used in this study that helped complete our research work.

REFERENCES AND NOTES

[1] Uredi, D.; Motati, D.; Watkins, E. Org Lett 2018, 20, 6336.
[2] Cam-Van, T. V.; Michael, U. L.; Jeffrey, W. B. Nat Chem 2014, 6, 310.
[3] Zumbragel, N.; Sako, M.; Takizawa, S.; Sasai, H.; Gröger, H. Org Lett 2018, 20, 4723.
[4] Bubun, B. Ultrason Sonochem 2017, 35, 15.
[5] Motati, D.; Uredi, D.; Watkins, E. Chem Sci 2018, 9, 1782.
[6] El-Wahab, A. H. F.; Mohamed, H. M.; El-Agrody, A. M.; El-Nassag, M. A.; Bedair, A. H. Pharmaceuticals 2011, 4, 1158.
[7] Faidallah, H. M.; Khan, K. A.; Makki, M. S. I. J Chinese Chem Soc 2011, 58, 191.
[8] Károlyházy, L.; Krajsovszky, G.; Farkas, L.; Boros, S.; Csámpai, A.; Mátyus, P. ARKIVOC, 2011, (ii), 18.
[9] Siddiqui, A.; Mishra, R.; Shaharyar, M.; Husain, A.; Rashid, M.; Pal, M.; Yathirajan, H. S. Mol Ther 2011, 717.
[10] Unsal tan, O.; Ozadali, K.; Yes, O.; Ilyurt, K. H.; Uzbay, T.; Balkan, A. Turk J Chem 2011, 35, 121.
[11] El-Hashash, M. A.; Darwish, K. M.; Rizk, S. A.; El-Bassiouny, F. A. Pharmaceuticals 2011, 4, 1032.
[12] Asif, M. Curr Med Chem 2012, 19, 2984.
[13] EL-Hashash, M. A.; Rizk, S. A.; El-Bassiouny, F. A.; Guirguis, D. B.; Khairy, S. M.; Guirguis, L. A. Egypt J Chem 2017, 60, 407.
[14] Azab, M. E.; Rizk, S. A.; Mahmoud, N. F. Chem Pharm Bull 2016, 64, 439.
[15] El-Hashash, M. A.; Rizk, S. A.; Darwish, K. M.; El-Bassiouny, F. A. Global J Health Sci 2012, 4, 162.
[16] Pathak, S.; Debnath, K.; Hossain, S. T.; Mukherjee, S. K.; Pramanik, A. Tetrahedron Lett, 201354, 3137.
[17] Al-Majedy, Y.;. K.; Al-Amiery, A. A.; Kadhum, A. A. H.; Mohamad, A. B. PLoS ONE 2016, 11, 1.
[18] Ming, B.; Xian-Qing, D.; Guo-Hua, G.; Cheng-Xi, W.; Zhe-Shan, Q. Med Chem 2013, 28, 792.
[19] Xue, D. Q.; Zhang, X. Y.; Wang, C. J.; Ma, L. Y.; Zhu, N.; He, P.; Shao, K. P.; Chen, P. J.; Gu, Y. F.; Zhang, X. S.; Wang, C. F.; Ji, C. H.; Zhang, Q. R.; Liu, H. M. Eur J Med Chem 2014, 85, 235.
[20] Munín, J.; Quezada, E.; Campos-Toimil, M.; Cano, E.; Uriarte, E.; Viña, D. Med Chem Res 2017, 26, 1682.
[21] Madhavan, G. R.; Chakrabarti, R.; Kumar, S. K.; Misra, P.; Mamidi, R. N.; Balraju, V.; Kasiram, K.; Babu, R. K.; Suresh, J.; Lohray, B. B. Eur J Med Chem 2001, 36, 627.
[22] Dong, C.; Liao, Z.; Xu, X.; Zhou, H. J Heterocyclic Chem 2014, 51, 1282.
[23] Romero, A. H.; Rodríguez, J.; García-Marchan, Y.; Leañez, J.; Serrano-Martín, X.; López, S. E. Bioorg Chem 2017, 72, 51.
[24] Magdy, M. G. Arch 2002, 6, 289.
[25] Safaei-Ghomi, J.; Shahbazi-Alavi, H.; Ziarati, A.; Teymuri, R.; Saberi, M. R. Chin Chem Lett 2014, 25, 401.
[26] Awadallah, F. M.; El-Eraky, W.; Saleh, D. O. Eur J Med Chem 2012, 52, 14.
[27] Wyman, R. V. Chem Rev 1948, 43, 447.
[28] Ghahremanzadeh, R.; Ahadi, S.; Sayyafi, M.; Bazgir, A. Tetrahedron Lett 2008, 49, 4479.
[29] Haider, N. Tetrahedron 1991, 47, 3959.
[30] Issac, Y.; El-Karim, E.; Donia, S.; Behalow, M. Sulfur Lett 2002, 25, 183.
[31] Yuhong, J.; Rajender, S.; Varma, A. J Org Chem 2006, 71, 135.
[32] Mohareb, R. M.; Al Farouk, F. O.; Wardakhan, W. W. Med Chem Res 2018, 27, 1984.
[33] Rizk, S.; Abdelwahab, S. S.; Sallam, H. A. J Heterocyclic Chem 2018, 55, 1604.
[34] Wang, H.; Cai, J.; Huang, H.; Deng, G. J. Org Lett 2014, 16, 5324.
[35] El-Hashash, M.; Rizk, S.; Atta-Allah, S. Molecules 2015, 20, 22069.
[36] Ananda, S.; Amarasekara, S. C. Org Lett 2002, 4, 773.
[37] Hwang, J. Y.; Choi, H.-S.; Gong, Y.-D. Tetrahedron Lett 2005, 46, 3107.
[38] Rizk, S. A.; Abdelwahab, S. S.; Elrazaz, E. J Heterocyclic Chem 2019, 56, 443.
[39] Vila, N.; Besada, P.; Costas, T.; Costas-Lago, M. C.; Teran, C. Eur J Med Chem 2015, 97, 462.
[40] Vollmer, W.; Tomasz, A. Infect Immun 2002, 70, 7176.
[41] Bera, A.; Biswas, R.; Herbert, S.; Kulauzovic, E.; Weidenmaier, C.; Peschel, A.; Gotz, F. J Bacteriol 2006, 189, 280.
[42] Elkholy, A.; Rizk, S.; Rashad, A. J Mol Struct 2019, 1175, 788.
[43] Rizk, S.; El-Naggar, A.; El-Badawy, A. J Mol Struct 2018, 1155, 720.
[44] Rizk, S.; Elsayed, G.; El-Hashash, M. J Iranian Chem Soc 2018, 15, 2093.

SUPPORTING INFORMATION

Additional supporting information may be found online in the Supporting Information section at the end of the article.